THE NUCLEAR SHIELDING SURFACE: THE SHIELDING AS A FUNCTION OF MOLECULAR GEOMETRY AND INTERMOLECULAR SEPARATION

CYNTHIA J. JAMESON
University of Illinois at Chicago
Department of Chemistry M/C-111
Chicago, Illinois 60680

ANGEL C. de DIOS
University of Illinois at Urbana
Department of Chemistry
Urbana, Illinois 61801

(dedicated to the memory of Thomas D. Bouman 1940-1992)

ABSTRACT. In making the connection between theoretical shielding values and experiments, it becomes necessary to consider medium effects and rovibrational averaging. The rovibrational averaging which takes the shielding for a molecule at its rigid equilibrium geometry into a thermal average shielding also provides the temperature dependence in the zero-pressure limit and the changes upon isotopic substitution which are experimentally accessible. The averaging of ^{15}N and ^{31}P shielding in the NH_3 and PH_3 molecules uses *ab initio* shielding surfaces and intramolecular potential surfaces or their derivatives. General trends are observed in comparing the shielding surfaces in these two molecules with H_2O and CH_4. A proper account of medium effects requires the knowledge of the intermolecular shielding surfaces, which are explored here for model systems ^{39}Ar in Ar...Ar, Ar...Ne, Ar...Na^+, Ar...NaH, and for ^{21}Ne in Ne...Ne and Ne...He, employing *ab initio* calculations (LORG and SOLO). The shapes of the shielding function $\sigma(R)$ for two atoms are shown to be similar for intra-and intermolecular shielding.

1. The Connection Between Experimental and Theoretical Shielding Values

Theoretical calculations of nuclear magnetic shielding provide the entire shielding tensor on an absolute basis, i.e., with respect to a bare nucleus. On the other hand, a measurement in the laboratory provides a chemical shift δ between the sample and the reference substance, i.e., a difference in shielding such as

$$\delta_A = \sigma(^{13}C, \text{TMS in } CDCl_3 \text{ soln. with A}, x_A, x_{TMS}, x_{CDCl_3}, 300K) - \sigma(^{13}C, \text{A in } CDCl_3 \text{ soln.}, x_A, x_{TMS}, x_{CDCl_3}, 300K) .$$

There are changes in shielding in going from the isolated molecule in its rigid equilibrium geometry to the single molecule at its ground vibrational state at 0 K, to the molecule in the gas at the zero-pressure-limit at 300 K, to the molecule in a gas at a given density, to the molecule in a neat liquid or a solution or a single crystal or powder.[1] As indicated in Fig. 1, these changes are not necessarily small.[2] They are not usually the same for

J. A. Tossell (ed.), Nuclear Magnetic Shieldings and Molecular Structure, 95–116.

the sample and the reference substance. Therefore, comparisons between theoretically calculated values of the absolute shielding tensor and the published chemical shift data in condensed phases can not be properly made. It is essential that experimental gas phase data be made available, especially for those nuclei in the first and second row of the periodic table, since the *ab initio* calculations are becoming sufficiently accurate for many of the molecules containing these nuclei. The absolute shielding scale is set by a measured spin rotation tensor for the nucleus in a (primary standard) molecule.[2-10] These are ^{13}C in CO molecule, ^{19}F in HF, ^{31}P in PH_3, ^{17}O in CO, ^{15}N in NH_3, ^{29}Si in SiH_4, etc. The measured chemical shift between molecule A and the primary standard molecule in the same sample in the gas phase provides the absolute isotropic shielding value for the nucleus in molecule A.

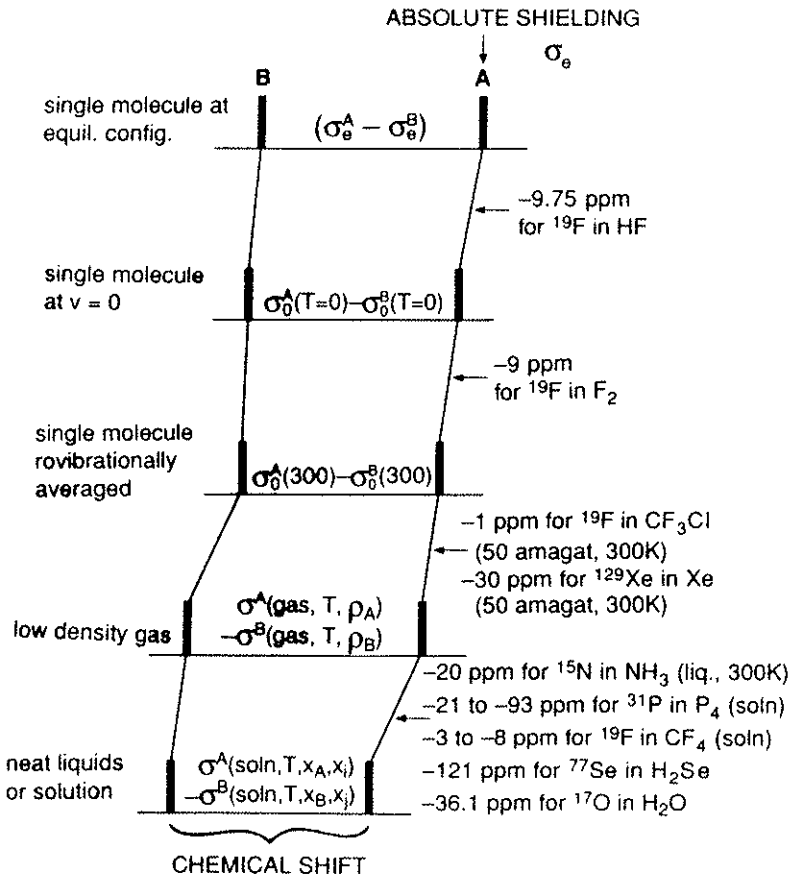

Fig. 1 Relation between the chemical shift and the absolute shielding at the equilibrium geometry

Ab initio calculations published in the last few years and those calculations being reported in this conference are reaching the level of accuracy such that even comparison with gas phase data may require some corrections for intermolecular effects and rovibrational averaging. We start with a gas phase experiment in which the nuclear shielding in a molecule in the pure gas is given by [11,12]

$$\sigma(T,\rho) = \sigma_0(T) + \sigma_1(T)\rho + \sigma_2(T)\rho^2 + \ldots \quad (1)$$

Experimentally, one can measure the temperature dependence of the shielding in the

molecule, $[\sigma_0(T) - \sigma_0(300\ K)]$, in the zero-pressure-limit.[13] The theoretical considerations of this are given in Section 2. Experimentally, one can also measure the density dependence of the shielding for the molecule in the gas phase; the terms $\sigma_1(T)\rho + \sigma_2(T)\rho^2 + ...$ can be obtained.[14] For example, the second virial coefficient of nuclear shielding for a pair of molecules can be determined by

$$\sigma_1(T) = -\left\langle \lim_{\rho \to 0} \left[\frac{\nu(T,\rho) - \nu_0(T)}{\nu_0(300\ K)} \right] \frac{1}{\rho} \right\rangle \tag{2}$$

from measurements in gas mixtures. Here, $\nu_0(T)$ is the resonance frequency in the limit of zero density. In a mixture of gases, both the $\sigma_1(T)$ for molecule A in the A-A pair and in the A-B pair can be determined.[15,16] The theoretical considerations of this are given in Section 3.

In making the corrections that bridge experiment with theory, we need companion mathematical surfaces. For *intermolecular* or medium effects, e.g., virial coefficients of shielding in the low density gas, or gas-to-liquid shifts, or solvent shifts, we need (a) the shielding surface as a function of the intermolecular coordinates, (b) the intermolecular potential energy surface in terms of the same intermolecular coordinates, and (c) the means of carrying out the averaging by some statistical mechanical means. For the dilute gas in the limit of density approaching zero, we need only the first term in the pair distribution function, exp[-V(R)/kT]. For example, for ^{129}Xe in xenon gas where V(R) is the Xe-Xe potential, the function $\sigma(R)$ is the shielding surface describing the ^{129}Xe shielding as a function of Xe-Xe distance, and $\sigma(\infty)$ is the value for an isolated atom, we have

$$\sigma_1(T) = \int_0^\infty 4\pi R^2\, dR[\sigma(R) - \sigma(\infty)]\exp[-V(R)/kT]\ . \tag{3}$$

For condensed phases or adsorbed species we need to carry out a grand canonical ensemble average, for example, and perhaps even include the many-body corrections.

For *intramolecular* rovibrational averaging effects, [17] e.g., the (v,J,K) dependence of shielding, or the temperature dependence of the thermal average shielding, and the mass dependence of shielding (isotope shifts), [18] we need (a) the shielding surface which is a function of molecular geometry, or as a function of nuclear displacement coordinates, (b) the intramolecular potential energy surface, or at least its higher derivatives with respect to displacements away from the equilibrium molecular geometry, and (c) the means of carrying out the averaging over the (v,J,K) states, e.g., by using the full anharmonic vibrational wave functions, [19] or by some other approach such as perturbation theory or by using a contact transformation which allows the averages to be expressed in terms of derivatives of the shielding surface and the derivatives of the potential energy surface.[17,20] Thermal averages are thereafter obtained by a statistical average over the thermally populated (v,J,K) states.[19,20] For example, the rovibrational average is

$$\langle\sigma\rangle_{vJK} = \int \psi^*_{vJK}(S_1, S_2, ...)\, \sigma(S_1, S_2, ...)\psi_{vJK}(S_1, S_2, ...)dS_1\, dS_2\ ... \tag{4}$$

for the shielding surface $\sigma(S_1, S_2, ...)$ in terms of nuclear displacement symmetry coordinates $S_1, S_2, ...$. The thermal average is given by:

$$\sigma_0(T) = \frac{\sum_{vJK} (2J+1)\, g_{NS}\, \langle\sigma\rangle_{vJK}\, \exp[-E_{vJK}/kT]}{\sum_{vJK}((2J+1)\, g_{NS}\, \exp[-E_{vJK}/kT]} \qquad (5)$$

In other words, the interpretation of experimental data at a fundamental level requires a knowledge of the shielding as a function of intermolecular distances and molecular geometry. We show some examples of each in this paper and in accompanying posters.

2. *Ab Initio* Calculations of Shielding Surfaces

Previous calculations of shielding in molecules at selected geometries displaced from equilibrium have been used to determine first and second derivatives of nuclear shielding in a wide variety of molecules.[21-26] However, only very few systematic studies of the shielding surface have so far been carried out. The first report of a full shielding surface was that of ^1H in the H_2^+ molecule by Hegstrom.[27] *Ab initio* calculations of ^{13}C and ^{17}O shielding in the CH_4 and in the H_2O molecules in the vicinity of their equilibrium geometries yield values of the surface along a variable symmetry displacement coordinate while maintaining the other symmetry displacements at zero.[21,28] When all such traces of the shielding surface are obtained, full rovibrational averaging can be carried out

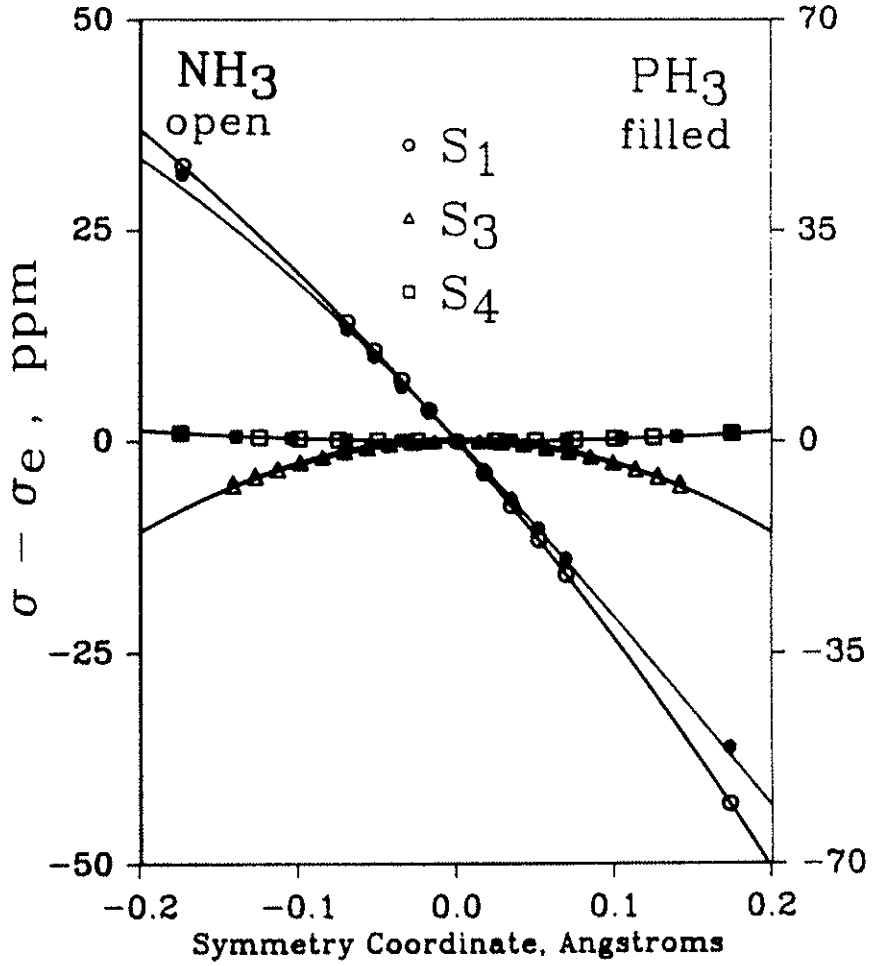

Fig. 2 Traces on the ^{15}N and ^{31}P shielding surfaces for NH_3 and PH_3.

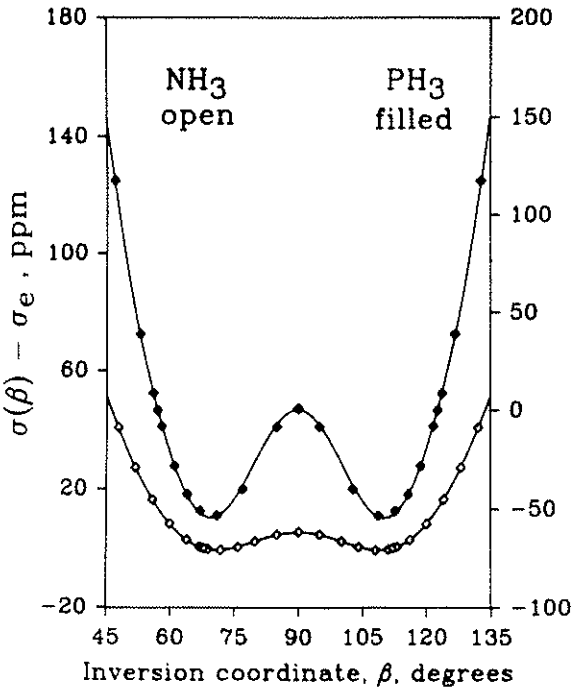

Fig. 3 Variation of the ^{15}N and ^{31}P shielding with inversion in NH_3 and PH_3.

to yield thermal average values, $\sigma_0(T)$, which can be compared with experiment.[19,29,30] Furthermore, the same rovibrational averaging in each of several isotopomers yields the shielding differences due to isotopic substitution (isotope shifts) which can also be compared with experiment.[19,29,30]

2.1 SHIELDING SURFACES FOR NH_3 and PH_3

We have recently reported the shielding surfaces of ^{15}N in NH_3 and ^{31}P in PH_3.[19,30] These are shown in Fig. 2 and 3. The symmetry coordinates are $S_1 = (1/\sqrt{3})\ (\Delta r_1 + \Delta r_2 + \Delta r_3)$, $S_{3a} = (1/\sqrt{6})\ (2\Delta r_1 - \Delta r_2 - \Delta r_3)$, $S_{4a} = (1/\sqrt{6}) r_e\ (2\Delta\alpha_1 - \Delta\alpha_2 - \Delta\alpha_3)$. The coordinates forming a degenerate pair with these (S_{3b} and S_{4b} respectively) provide exactly the same traces as S_{3a} and S_{4a}. The remaining coordinate S_2 is the symmetric bend. Since this corresponds to the inversion coordinate over which full averaging takes place at room temperature in NH_3, a more extensive portion of the surface has been calculated so as to include angles from 45° to 135° for the NH or PH bond relative to the C_3 symmetry axis of the molecule.

In this work the shielding calculations were performed with RPAC Version 8.5 program [31] by Hansen and Bouman [32] which employs the localized orbital local origin (LORG) method while GAUSSIAN88 provided the necessary SCF information.[33] The computations were carried out in an IBM 3090/300J/vector facility. The basis set employed is relatively large: three sets of d-type polarization functions on the apex atom and two sets of p-type polarization functions on the hydrogen were added to the 6-311+G basis of Pople.

Fig. 2 shows that when the vertical scales (^{31}P and ^{15}N shieldings) are related by the ratio of $\langle a_0^3/r^3\rangle_{np}$ for P and N atoms, the surfaces are very close to being superposable,

except for the inversion coordinate. The traces on the shielding surface with respect to the inversion coordinate in Fig. 3 have similar shapes to the potential energy surface. However, the barrier in the PH_3 molecule is much much higher than that for NH_3 so that in the averaging over the inversion coordinate all the shielding values from 45° to 135° need to be considered in NH_3 whereas the S_2 coordinate in PH_3 can be treated in the normal way as with all other coordinates, assuming small displacements. The NH_3 inversion wavefunctions were obtained from numerical solution of the Schrödinger equation for inversion, [19] using the empirical potential surface that was fit to high resolution spectra of all isotopomers of NH_3 by Spirko et al.[34] The results of the thermal averaging are in very good agreement with the experimental data for the $[\sigma_0(T) - \sigma_0(300\ K)]$ measured recently for NH_3 and PH_3, [19,30] and the isotope shifts $[\sigma(PD_3) - \sigma(PH_3)]$ and $[\sigma(ND_3) - \sigma(NH_3)]$ are in reasonable agreement with experiment. Details of this work can be found in ref [19] and [30].

2.2 GENERAL TRENDS

We can compare our results for NH_3 and PH_3 in Fig. 2 with the other shielding surfaces for CH_4 and H_2O, that have been previously reported by W. T. Raynes and

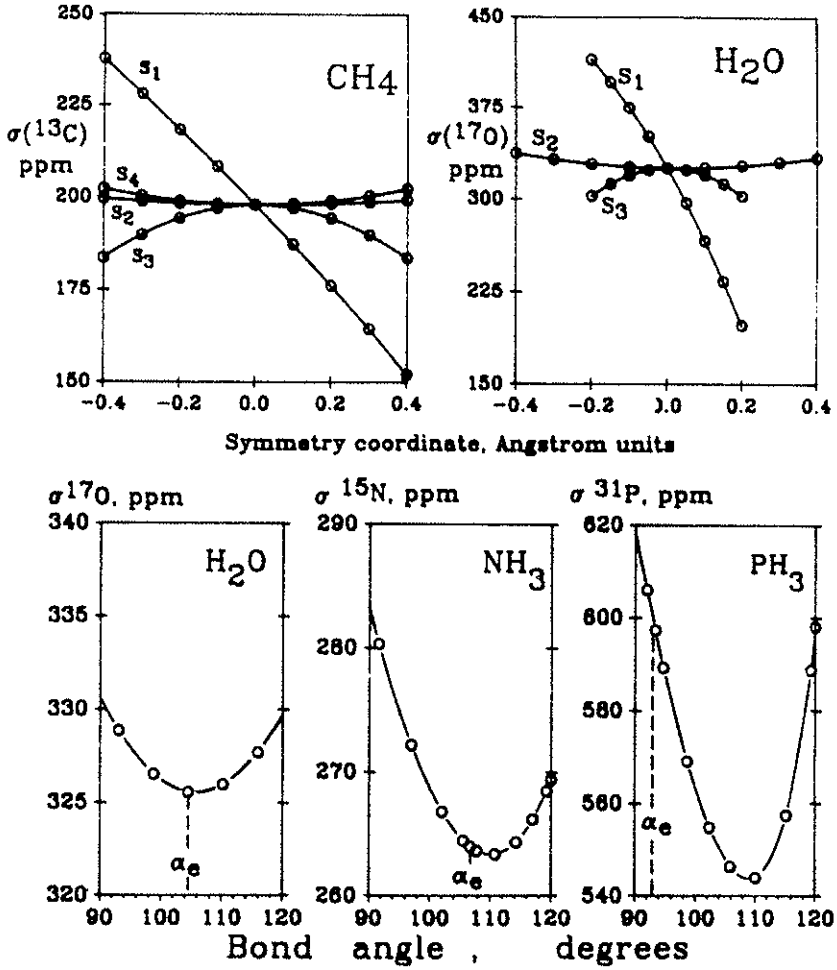

Fig. 4 Traces on the shielding surfaces of CH_4 and H_2O. Comparison of bond angle dependence

coworkers.[21,29] The latter are shown in Fig. 4. For the hydrides, at least, the shielding surfaces look strikingly similar. The symmetric stretch (S_1) leads to deshielding of ^{15}N, ^{31}P, ^{13}C, and ^{17}O in these molecules. The trace along the asymmetric stretch is concave downward (deshielding), whereas the trace along the asymmetric bend is concave upward (toward increased shielding). The asymmetric stretch corresponds to larger changes in shielding than the asymmetric bend but since the vibrational frequencies are greater for the stretch than the bend, the effects on the thermal average nearly cancel. The shielding trace along the symmetric bond angle change (or inversion) in OH_2, NH_3, and PH_3 are all concave upward and the shielding value is minimum at very nearly the tetrahedral angle in all cases. However, the equilibrium bond angle is close to tetrahedral in OH_2 and NH_3 but is 93° in PH_3. Therefore, in the former, the symmetric bond angle changes lead to uniformly higher shielding whereas in PH_3, the linear term in this coordinate leads to *deshielding* while the quadratic term leads to increased shielding with increasing temperature.

Another point of similarity is that in all these systems the largest contribution to the isotope shift, $[\sigma^X(XD_n) - \sigma^X(XH_n)]$, comes from the symmetric stretch. The thermal averages in Fig. 5 show very similar trends. In these hydrides, the thermal average shielding, $\sigma_0(T)$ decreases with increasing temperature, although much less pronounced in CH_4 and NH_3. The bond angle contributions in all 4 molecules make the calculated

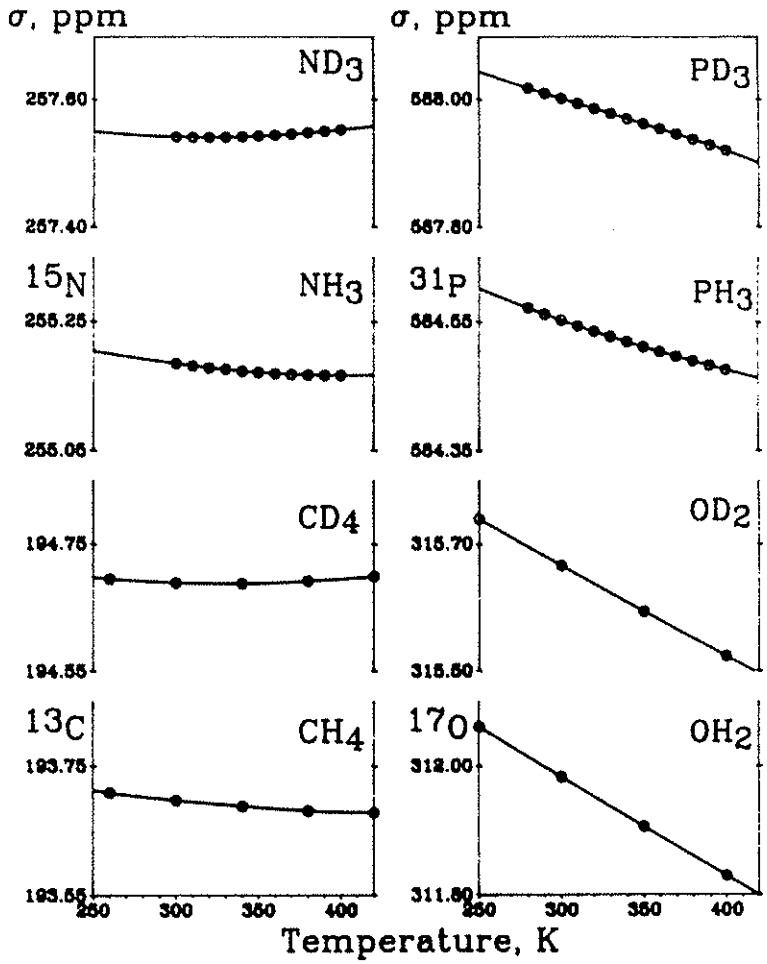

Fig. 5 Thermal average shielding $\sigma_0(T)$

$\sigma_0(T)$ functions concave upward† and this becomes more pronounced for the deuterated versions.

Although the theoretical shielding values decrease with bond extension in most molecules, and most of the experimental evidence (isotope shifts and temperature dependence of shielding) point toward deshielding upon bond extension, there are, however, theoretical cases of increasing shielding upon bond extension. The first example was reported for LiH by Stevens and Lipscomb[36] and Ditchfield.[25] Furthermore, D. B. Chesnut[22] has discovered a fascinating variation of $(\partial\sigma^X/\partial R)_{eq}$ in XH_n across the periodic table, positive for hydrides LiH and BeH_2, becoming increasingly negative toward FH. Similarly it is positive for NaH, MgH_2, and AlH_3, becoming increasingly negative toward ClH. A smooth algebraic change in $(\partial\sigma^X/\partial R)_{eq}$ occurs as X moves across the periodic table, tracing out an arch in each row with X = Be and Mg at the most positive value. At the end of this paper we will offer a reasonable explanation for this fascinating trend.

3. Intermolecular Shielding

Excepting molecular beam studies, the application of NMR to the elucidation of molecular structure and mechanisms of molecular reactions nearly always involves observations of the molecules in some medium, whether in gas, liquid, solid, or adsorbed phases. An understanding of the intermolecular effects on nuclear magnetic shielding is crucial to taking proper account of solvent effects, or conversely, to using the NMR chemical shift as a probe of intermolecular interactions. There is a large body of gas phase data [37] which provides information on the intermolecular contributions to the chemical shift; the observed signs, magnitudes, and the dependence on temperature need to be accounted for. Apart from the bulk susceptibility shifts which are present in all samples, there are true intermolecular shifts that can be attributed to polar and hydrogen-bonding effects and magnetic anisotropy of neighbor molecules (as in aromatic solvents). These have well-understood mechanisms and will not be discussed further here. The enigmatic part of the intermolecular shielding is that which gives rise to what had been termed van der Waals shifts.[38] This is the subject of this Section.

The study of the intermolecular shielding function, the change in the nuclear shielding as a function of the distance between interacting molecules and their orientation, is of fundamental importance in its own right. The intermolecular shielding function in general has important dependence on orientations of the interacting molecules. However, we start with the simplest case of two interacting rare gas atoms and focus attention on the dependence of the shielding on the intermolecular separation R. Therefore, within this article, we will refer to the intermolecular shielding function as $\sigma(R)$.

3.1 ^{29}Ar AS A MODEL SYSTEM

In principle, the behavior of the intermolecular shielding function of two rare gas atoms at the two limits is well known. The separated atoms is the reference limiting situation; the

---

†This is not generally the case. In the diatomic molecules (such as ^{1}H in H_2^+ or H_2, ^{19}F in HF or F_2) and for ^{19}F in a large number of fluorides, [35] the $\sigma_0(T)$ functions are concave downward and strongly decreasing (deshielding) with increasing temperature. The shielding of end atoms are largely dependent on the bond stretch and much less sensitive to bond angle changes.

diamagnetic shielding in a free atom is well known. When the interacting atoms correlate with a united atom S state, as Ar + Ar does with the Kr ground state, the shielding of the united atom is also well known, a purely diamagnetic shielding.[39] Thus, $[\sigma(R) - \sigma(\infty)]$ the intermolecular shielding relative to the separated system was known for Ar-Ar to be [σ(free Kr atom) - σ(free Ar atom)] at R = 0, and was known to be zero at R = ∞. In the intermediate region, the general shape of the function was unknown.

For calculations of intermolecular shielding, it is even more important to damp out the errors which result from incomplete cancellation of large positive and negative long-range contributions. In calculations of magnetic properties, this is known as a gauge origin problem. Furthermore, since the long-range interaction between two rare gas atoms is a result of electron correlation, we need to investigate any additional contributions from electron correlation beyond the coupled Hartree-Fock or random phase approximation (RPA) level of theory. For these reasons, we choose a local origin method that effectively damps out the errors in calculating the long-range contributions to the diamagnetic and paramagnetic terms and which can be extended to include second-order correlation contributions. We used the localized orbital local origin (LORG) method developed by Hansen and Bouman [32] and the second order LORG (SOLO) approach, in which the energy matrices and transition moments are evaluated such as to retain all terms through second order in electron correlation, i.e., using $\Omega^{(2)}$ and $t^{(2)}$.[40] The second-order effects on the diamagnetic terms have not been included in this calculation. These have been shown to be small, even for molecules such as CO and N_2 for which a correct description requires more than one determinant. For these molecules, the diamagnetic shielding results from configuration interaction (CI) calculations differ by less than 2 ppm from the self-consistent field (SCF) results for all nuclei.[41,42]

The SOLO calculations were carried out with the help of Professor T. D. Bouman using GAUSSIAN 90 [33] to generate the SCF molecular orbitals, and the RPAC 9.0 molecular properties programs system [43] implemented on the Cray 2 of the National Center for Supercomputing Applications at the University of Illinois, Urbana.

The use of counterpoise or ghost orbitals [44] would reduce the bias that results if the pair basis represents the wave function of Ar_2 in the simultaneous fields of the external magnet and the nuclear moment more accurately than the single atom basis represents the wave function of an isolated Ar atom in the presence of the two fields. Since the chemical shielding is a localized property (the shielding field produced by an electron is proportional to the inverse cube of the distance of the electron from the observed nucleus), basis set superposition errors are expected to be negligible even in this case where the intermolecular effects on shielding are being sought. Nevertheless, to verify this expectation, we carried out calculations of the single Ar atom at the 6-311G (3*d*) level with and without an equal number of ghost orbitals at various internuclear distances. We have established that the ghost orbital contribution is entirely negligible in this system.

The LORG and SOLO results for Ar_2 [45] are shown in Fig. 6. A numerical comparison at selected distances is shown in Table 1 for the LORG vs. SOLO results. This is the first *ab initio* intermolecular σ(R) function that has been calculated for a range of values of internuclear separations wide enough to show the shape of the function, and which is consistent with the correct limit at R = 0. The behavior at extremely short distances ~1Å or shorter can become very complicated because of avoided curve crossings with other states of the same symmetry. In any case, these regions are not sampled at the modest temperatures and pressures at which the gas phase experiments have been carried out.

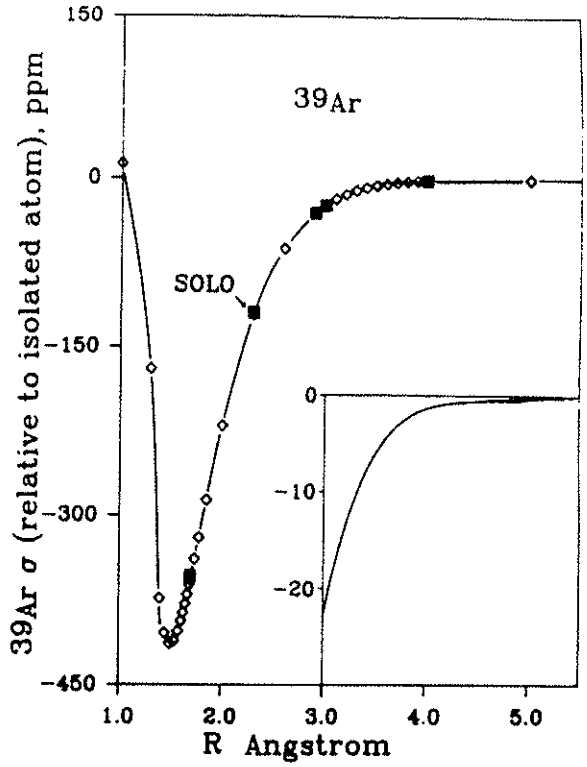

Fig. 6 ^{39}Ar shielding in the Ar...Ar system

TABLE 1. ^{39}Ar shielding in Ar_2 at two levels of calculation, with (SOLO) and without (LORG) second order correlation. [45]

$R_{Ar\text{-}Ar}$(Å)	[σ(R) - σ(∞)](ppm)	
	LORG	SOLO
1.70	-356.90	-353.49
2.30	-121.39	-119.64
2.90	-30.32	-30.68
3.00	-23.53	-23.91
4.00	-1.30	-1.40
5.00	-0.04	-0.00

TABLE 2. ^{39}Ar shielding in Ar...Na^+ [45]

$R_{Ar\text{-}Na+}$ (Å)	[σ(R) - σ(∞)](ppm)	
	LORG	SOLO
1.50	-42.60	-62.85
1.56	-39.78	-60.78
3.20	-4.77	-5.55

3.2 THE R-DEPENDENCE OF INTERMOLECULAR SHIELDING

SOLO includes both dispersion and overlap/exchange contributions and their interaction. However, at large distances, the intermolecular shielding is the small difference between two large terms and thus is difficult to obtain accurately. Therefore, the exact R-dependence at long range, the coefficients of the R^{-6} and R^{-8} terms in the *ab initio* shielding function $[\sigma(R) - \sigma(\infty)]$ cannot be determined accurately. For intermediate distances, a plot of log $[(\sigma(\infty) - \sigma(R))/\text{ppm}]$ vs. log (R/Å) in the range of distances (0.5 - 1.0) times the r_{min} of the Ar_2 potential function gives a slope equal to -6.67, i.e., $[\sigma(R) - \sigma(\infty)]$ behaves as $R^{-6.67}$. In this range of separations $[\sigma(R) - \sigma(\infty)]$ for ^{39}Ar in Ar ... Ne behaves as $R^{-6.79}$, ^{21}Ne in Ne... Ne behaves as $R^{-6.74}$, and ^{21}Ne in Ne... He goes as $R^{-7.41}$.[46]

A simple physical explanation for the R dependence of $[\sigma(R) - \sigma(\infty)]$ from *ab initio* calculations in rare gas pairs over the range of R values from $0.7r_0$ to $3\text{-}4r_0$ is as follows: The dispersion interaction causes a buildup of charge in the region between the two nuclei. The R^{-6} dispersion energy arises from the classical electrostatic attraction of each nucleus to its own dipolar electron cloud.[47] At the same time the R^{-6} shielding term due to dispersion arises from the paramagnetic shielding of a dipolar electron cloud. Similarly, the mutual distortion of the two atoms due to overlap leads to dipolar electron clouds, and the overlap dipole varies exponentially with R at very short range. The R^{-6} to R^{-8} dependence of shielding due to overlap arises from the paramagnetic shielding of a dipolar electron cloud.

There is a somewhat different behavior of the shielding with separation when electrical charges are involved. For example, let us compare ^{39}Ar shielding in Ar...Ne with that in Ar...Na^+ in Fig. 7. We find that approach of $\sigma(R)$ to the separated atoms value is

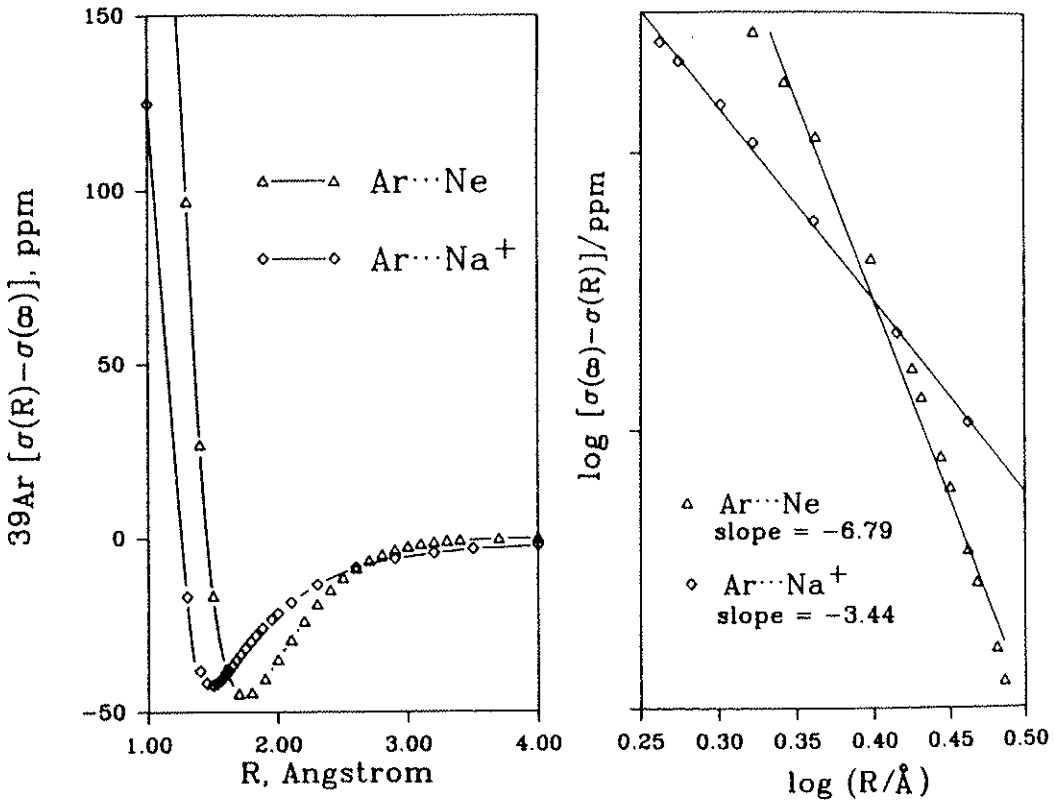

Fig. 7 ^{39}Ar shielding surfaces for the isoelectronic systems Ar...Ne and Ar...Na^+

approximately $R^{-3.44}$ for ^{39}Ar in Ar...Na^+ for $R \geq 1.8$Å whereas it is the typical (for rare gas pairs) approximately $R^{-6.79}$ for ^{39}Ar in Ar...Ne for $R \geq 2.0$Å. An understanding of this different R dependence at large R can be gained from the expected functional forms of $\sigma(R)$ in the long-range limit.

The long-range limiting behavior in these systems can be modeled by considering the effects of the neighboring atom or ion on the ^{39}Ar shielding in terms of the electric fields F_γ created by the neighbor at the position of the ^{39}Ar nucleus. In the presence of an applied electric field the shielding can be written as: [48-50]

$$\sigma_{\alpha\alpha} = \sigma_{\alpha\alpha}^{(0)} + \left(\frac{\partial\sigma_{\alpha\alpha}}{\partial F_\gamma}\right)_{F_\gamma=0} F_\gamma + \left(\frac{\partial^2\sigma_{\alpha\alpha}}{\partial F_\gamma \partial F_\beta}\right)_{F_\beta=F_\gamma=0} F_\gamma F_\beta + .. \tag{6}$$

We may further include the effects of electric field gradients $F_{\gamma\beta}$. For an Ar atom, the shielding first derivatives with respect to the electric field (the shielding polarizability, a term coined by Dykstra [51,52]) vanish by symmetry,

$$\left(\frac{\partial\sigma_{\alpha\alpha}}{\partial F_\gamma}\right)_{F_\gamma=0} = 0. \tag{7}$$

If we are observing only the isotropic shielding, then the 1-2 pair at a fixed separation R is considered to be tumbling freely in the magnetic field B_0 and the contributions of electric field gradients to $[\sigma_{iso} - \sigma_{iso}^{(0)}]$ for an Ar atom vanish also.

Therefore, in the mean field model of Raynes, Buckingham, and Bernstein, [12] where the neighbor atom effects on the shielding are considered in terms of the mean square electric fields $\overline{F^2}$ it produces at the nucleus in question,

$$\left[\sigma_{iso} - \sigma_{iso}^{(0)}\right]_{\substack{long-\\range}} \approx \frac{1}{3}\left\{\frac{1}{2}\sigma_{zz,z,z}^{(2)} + \sigma_{zz,x,x}^{(2)}\right\}_{Ar} \overline{F^2} \tag{8}$$

where $$\sigma_{zz,x,x}^{(2)} \equiv \left(\frac{\partial^2\sigma_{zz}}{\partial F_x^2}\right)_{F_x=0} \tag{9}$$

and $$\overline{F^2} = q_2^2 R^{-4} + \mu_2^2 R^{-6}(3\cos^2\theta+1) + \frac{9}{8}\Theta_2^2 R^{-8}(1-2\cos^2\theta+5\cos^4\theta)$$
$$+\left[-\frac{C_6}{\alpha_{Ar}(0)} R^{-6} - \frac{R^{-8}}{\alpha_{Ar}(0)}\left(C_8 - 5C_6\frac{C_2}{\alpha_2(0)}\right) - ...\right] \tag{10}$$

Here, for Ar with a linear molecule, for example, q_2, μ_2, and Θ_2 are the electric charge, dipole moment, and quadrupole moment of the neighbor (2), and $\alpha_2(0)$ and C_2 are its static electric dipole polarizability and quadrupole polarizability.[53] The angle between the axis of molecule 2 and the intermolecular axis is θ. The dispersion energy coefficients for the 1-2 pair are C_6 and C_8. The dispersion term in the mean square field (in square brackets) is that given by Buckingham and Clarke.[54]

Indeed, we find the appropriate interpretation for the R^{-4} tail shown by the *ab initio* ^{39}Ar shielding in the Ar...Na^+ system. On the other hand in Fig. 8, as expected, a near $\sim R^{-6}$ tail is found for Ar...NaH (collinear). Note too how the additional electrons in NaH makes a difference in the short/intermediate range behavior of the shielding of Ar.

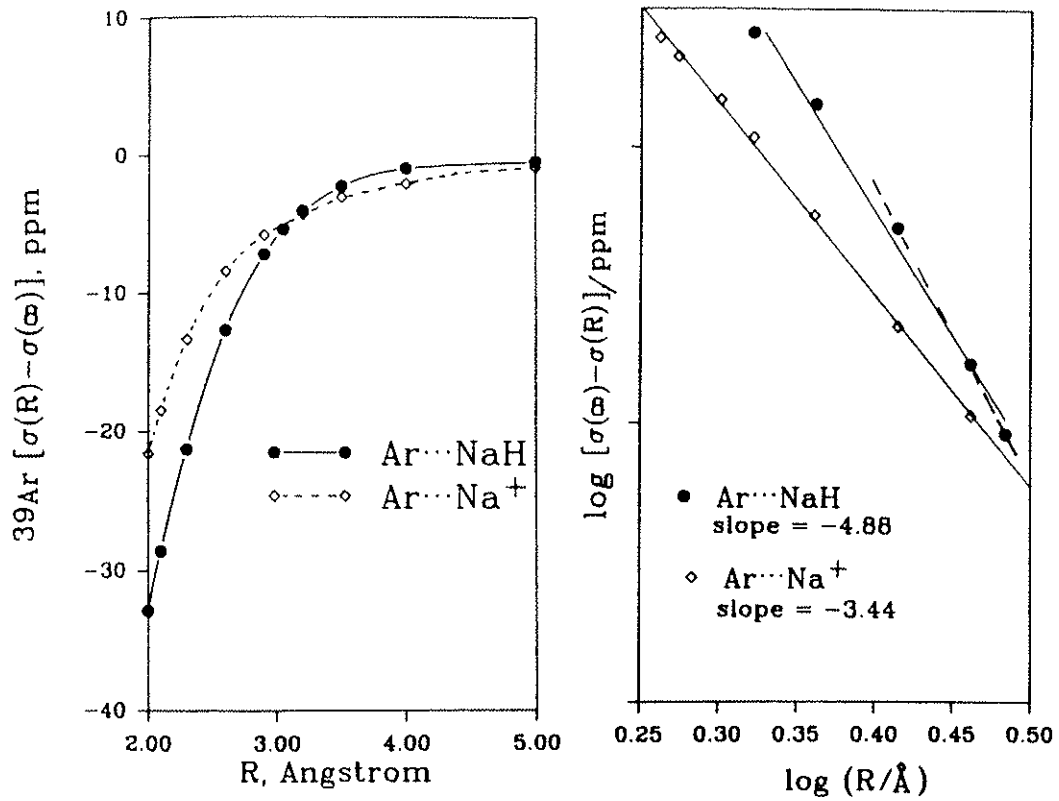

Fig. 8 ^{39}Ar shielding surface for Ar...Na$^+$ compared with Ar...NaH (collinear)

Only *ab initio* calculations can provide the behavior of σ(R) over a wide range of separations. However, by using simple physical models, we conclude that we have a reasonably good understanding of the R-dependence of the intermolecular shielding function.

3.3 SCALING OF THE INTERMOLECULAR SHIELDING FUNCTION

A possible scaling of intermolecular shielding functions for the rare gas pairs is suggested by the long-range limit form of the function.[45] In the mean field model, the mean square effective field, created at 1 due to the dispersion interaction between 1 and 2, can be related to the dispersion energy of the pair of interacting atoms as in Eq. (10):[54]

$$\overline{F^2} = -\frac{C_6}{\alpha_1(0)} R^{-6} - \frac{R^{-8}}{\alpha_1(0)} \left(C_8 - 5C_6 \frac{C_2}{\alpha_2(0)} \right) - \ldots \qquad (11)$$

In the simpler London approximation, the mean square field at 1 due to 2 is [55,56]

$$\overline{F^2} \approx \frac{3}{2} \alpha_2(0) \frac{U_1 U_2}{U_1 + U_2} R^{-6} \qquad (12)$$

where U_1 and U_2 are the ionization potentials and α(0) is the static polarizability. Although the mean field model may not be strictly valid at distances shorter than r_{min} of the potential function, the factors appearing in the above expression suggest that an approximate scaling of the shielding functions may be possible. Furthermore, the nature of

the shielding hyperpolarizability,

$$\left(\frac{\partial^2 \sigma}{\partial F^2}\right)_{F=0} = \frac{1}{3}\left\{\frac{1}{2}\,\sigma_{zz,z,z}^{(2)} + \sigma_{zz,x,x}^{(2)}\right\} \tag{13}$$

suggests scaling factors $\langle a_0^3/r^3\rangle \cdot \alpha_1(0)$. It is well known that the magnitudes of NMR chemical shifts of nuclei across the Periodic Table scale as $\langle a_0^3/r^3\rangle_{np}$ for the free atom in question, [57] a quantity which can be derived directly from the spin-orbit splittings observed in atomic spectra. In other words, the sensitivity of the nuclear shielding to changes in the electronic environment of the nucleus, e.g., in going from one molecule to another, has been found to be reflected by $\langle a_0^3/r^3\rangle_{np}$. The distortion of the electronic distribution of an atom in the presence of a static uniform electric field depends on the static electric dipole polarizability of the atom. Thus, the shielding hyperpolarizability is expected to scale as $\langle a_0^3/r^3\rangle_{np} \cdot \alpha(0)$. We have therefore suggested that the scaling factors relating intermolecular shielding functions of rare gas pairs are [45]

$$\langle a_0^3/r^3\rangle_1\, \alpha_1(0) \cdot \frac{3}{2}\alpha_2(0)\,\frac{U_1 U_2}{U_1 + U_2}.$$

For example, at long-range separations,

$$[\sigma(^{129}\text{Xe in Xe ... Kr}) - \sigma(\infty)] \approx \frac{\langle a_0^3/r^3\rangle_{Xe}\ \alpha_{Xe}(0)\,\alpha_{Kr}(0)}{\langle a_0^3/r^3\rangle_{Ar}\ \alpha_{Ar}(0)\,\alpha_{Ar}(0)}\ \frac{U_{Xe}\ U_{Kr}}{U_{Xe} + U_{Kr}}\ \frac{2}{U_{Ar}}$$

$$\times\, [\sigma(^{39}\text{Ar in Ar...Ar}) - \sigma(\infty)]_{\substack{ab \\ initio}} \tag{14}$$

There are no adjustable parameters here.

We have some evidence that these factors provide a successful scaling of the intermolecular shielding in rare gas pairs, in the range of values $R \geq 0.7\ r_0$. One is the nearly conformal R dependence of the shielding for all rare gas pairs for which we have carried out *ab initio* calculations: ^{39}Ar in Ar...Ar, Ar...Ne, ^{21}Ne in Ne...Ne, and Ne...He exhibit $\sim R^{-6.67}$, $\sim R^{-6.79}$, $\sim R^{-6.74}$, and $\sim R^{-7.41}$ behavior, respectively in this range of separations.[46] This indicates that the shielding functions are conformal and scaling is possible. Secondly, the *ab initio* ^{21}Ne shielding in Ne...Ne is closely reproduced by the *ab initio* ^{39}Ar shielding in Ar...Ar when the latter is multiplied by the scaling factors given above. This is shown in Fig. 9. Thirdly, the range of gas-to-solution shifts of ^{129}Xe, ^{83}Kr, and ^{21}Ne atoms in the same set of solvents spanning a range of dielectric constants do form a straight line passing through the origin when plotted against $\langle a_0^3/r^3\rangle \cdot \alpha(0) \cdot U$.[45] Finally, the scaling factors have been used to convert the *ab initio* $[\sigma(R) - \sigma(\infty)]$ for ^{39}Ar in Ar...Ar into the corresponding values for ^{129}Xe in Xe...Ar, Xe...Kr, and Xe...Xe. These can be used to calculate the second virial coefficients of shielding

$$\sigma_1(T) = \int_0^\infty 4\pi R^2\, dR[\sigma(R) - \sigma(\infty)]\ \exp\,[-V(R)/kT].$$

These values are compared with the gas phase experimental data in Fig. 10. The agreement is satisfactory. The experimental signs, orders of magnitude, and temperature dependences are well-reproduced. The appropriate scaling of the internuclear distance is unknown but we chose r_0 for convenience, as suggested by the conformal interaction potential energy functions for rare gas pairs which are scaled by r_0 and ϵ.[58]

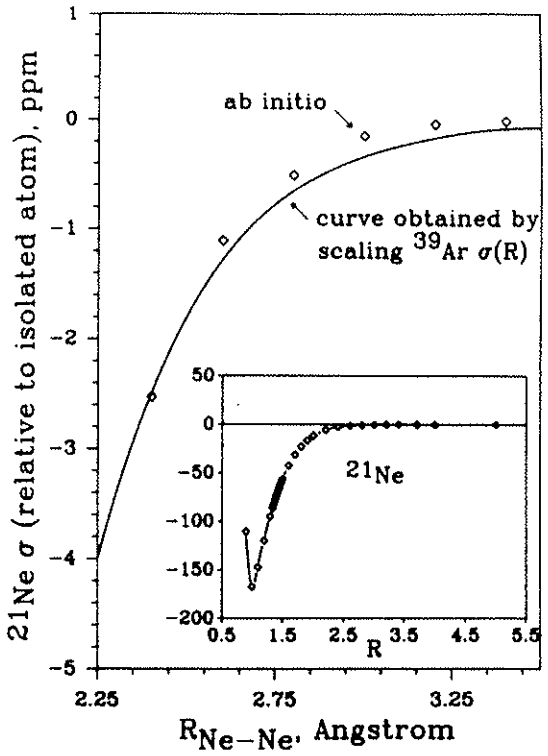

Fig. 9 ^{21}Ne shielding in Ne...Ne compares well with scaled Ar...Ar

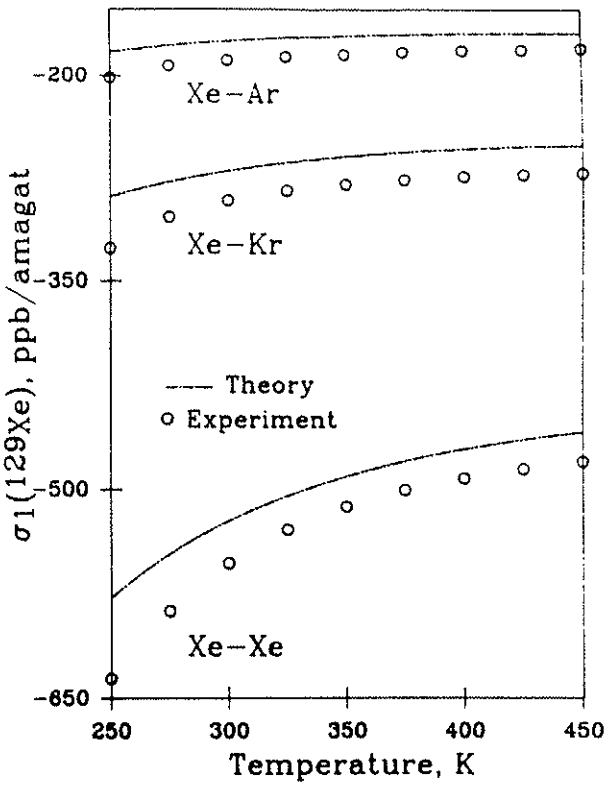

Fig. 10 Second virial coefficients of ^{129}Xe shielding from ^{129}Xe $\sigma(R)_{Xe\text{-}X}$ obtained by scaling $\sigma(R)_{Ar\text{-}Ar}$.

4. The General Shape of the Shielding Function

All the *ab initio* intermolecular shielding surfaces that we have found (Ar...Ar, Ar...Ne, Ne...Ne, Ne...He, Ar...Na^+, and Ar...NaH) have the general shape like that of a potential energy function for rare gas pairs.[46] We propose that this shape is the general qualitative shape of an intermolecular shielding function. Some facts concerning σ(R) require the existence of a negative minimum in the function [σ(R) - σ(∞)] for Ar_2 and predominantly negative values in the well region of the V(R). (a) The united atom is Kr which has a known large diamagnetic shielding which is 2.6 times that of σ for an isolated Ar atom.[39] (b) The observed second virial coefficients of shielding in nearly all systems studied in the gas phase is *negative* with few exceptions.[37] (c) The distortion asssociated with the long-range dispersion forces provides a negative [σ(R) - σ(∞)].

In every case the R dependence in the range of separations inside of r_{min} is close to R^{-6} to R^{-8} (except in Ar...Na^+ where there is an obvious long-range ~R^{-4} dependence that is expected for the system). In the presence of an electric dipole (the Ar...NaH system) the R dependence approaches R^{-6} once again, not unexpected from Buckingham's mean square field approach.[12] It is interesting that for the intermediate range of distances (between 0.8 r_0 and r_{min}) the R dependence is still about the same as might be expected from the dispersion contributions predicted by the mean square field model of Buckingham. SOLO calculations which include second order electron correlation contributions to shielding provide only a small correction in this range of distances.[45]

The shapes of the intermolecular shielding functions are similar to the *intra*molecular

shielding function for ^1H in H_2^+ molecule. Interestingly (we don't know the fundamental basis for it yet), the very accurate proton shielding in the H_2^+ molecule has an $R^{-6.0}$ behavior for R values greater than that which corresponds to the mininum in the shielding function, for distances 8 a.u up to 20 a.u. Ergo, we propose that all two-atom shielding functions involving ^1S states have the *same qualitative* shape, that is, if we do not include electron spin or the natural paramagnetism of separated atom states which have non-zero angular momentum. (For example, if HF were to separate to the F^- and H^+ ions then we would have ^1S separated atom states.)

What do shielding functions in diatomic molecules (other than ^1H in H_2^+) look like? *Ab initio* calculations in the vicinity of the equilibrium geometry are well-known for H_2, HF, HCl, NaH, LiH, CO, N_2, but a wide range of R values have not been investigated. If indeed a universal qualitative shape is that which we have found for intermolecular shielding, we should be able to locate a shielding minimum. For most molecules the shielding derivative with respect to bond extension is *negative*. Thus the shielding minimum, if it exists, will be found at R values much greater than the equilibrium bond length. Unfortunately, at very large separations the orbital paramagnetism of the non- ^1S separated atom states comes into play. This paramagnetism is of course not included in the frequently quoted diamagnetic shielding for the free atom.[39] When the separated atom states are not ^1S, the shielding just keeps on being larger negative with increasing bond length.

We can however, search for a shielding minimum at R values shorter than the equilibrium bond length, if the derivatives of the shielding at the equilibrum geometry is positive. Possible candidates are NaH and LiH. We did not reach the shielding minimum in LiH even at R = 0.5Å. However, we were able to calculate ^{23}Na shielding in the NaH molecule over a wide range of R values, [46] and what we found is shown in Fig. 11. This too is a shielding function of the same general shape that we have seen before.

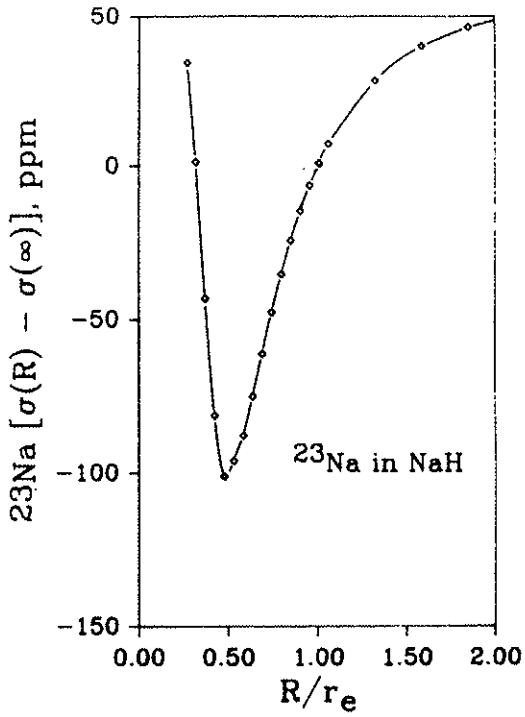

Fig. 11 The ^{23}Na shielding surface in the NaH molecule

The shielding that is observed experimentally depends on the relevant region over which the averaging takes place. In Fig. 12 we attempt to show the relationships between the portion of the σ(R) function that is of importance, and the potential energy function V(R) which governs the averaging over the appropriate range of R values. The unit of energy in each subfigure is Kelvins, to indicate which portion of the potential function becomes relevant in the sampling of σ(R) at any given temperature. The progression of the "active" range of R values across the σ(R) function in going from ^{1}H in the H_2^+ molecule, to ^{23}Na in the NaH molecule, to ^{39}Ar in $ArNa^+$ and in Ar_2 provides different samplings of generally the same shape of σ(R) function.

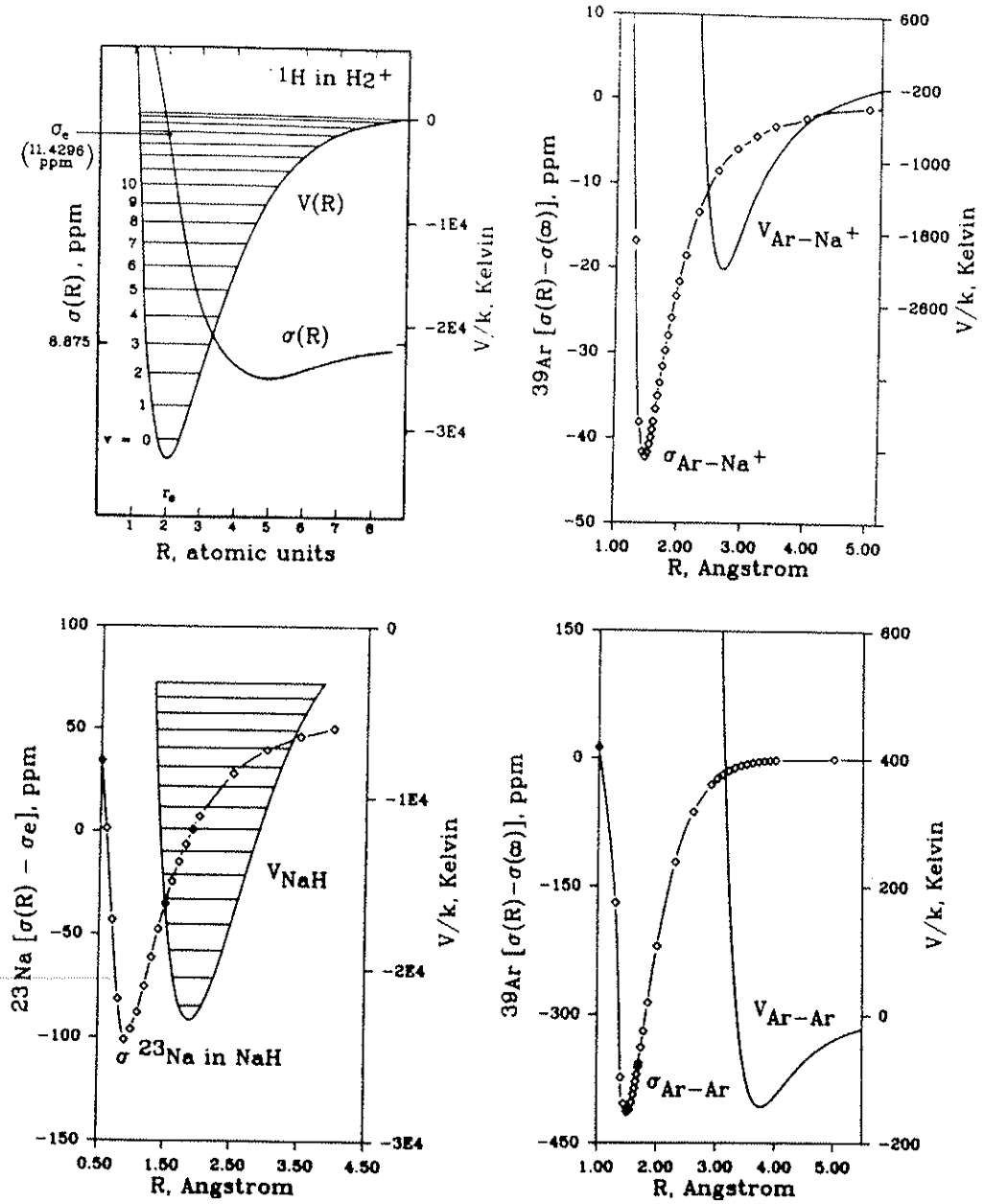

Fig. 12 Comparison of inter- and intra-molecular shielding surfaces

Although we cannot calculate the entire shielding function for nuclei in most diatomic molecules (for reasons stated earlier), we believe that they *all* nevertheless have shapes similar to those shown in Fig. 12 (excluding contributions from orbital paramagnetism in non-S systems). We propose that even for those diatomic molecules for which we are unable to calculate $\sigma(R)$ over a wide enough range of separations (without encountering the problems cited above), the shape of the shielding function is qualitatively similar to that we found for the intermolecular case of Ar in Ar_2. Evidence for this assertion is provided by the shape of the shielding function in the vicinity of the equilibrium geometry: The second derivatives in both the extremes (that is, large negative first derivative and positive derivatives corresponding to the extreme ends of a row in the Periodic Table) are negative. ^{39}Ar in Ar_2 does have negative second derivatives at the small R side (where it has a large negative first derivative) and the large R side of the shielding minimum (where it has a positive first derivative). In the immediate vicinity of r_e the *ab initio* (LORG) shielding functions for diatomic molecules are remarkably similar for analogous diatomic molecules. If we scale them by $\langle a_0^3/r^3\rangle \cdot r_e$, the comparison can be made directly. We find that $[\sigma(R) - \sigma(\infty)]/\langle a_0^3/r^3\rangle r_e$ for ^{35}Cl in ClF and ^{19}F in F_2 are nearly exactly superposable in the range of R values corresponding to the classical turning points of the ground vibrational states of these molecules.[46] The same remarkable superposability is found for ^{35}Cl in HCl and ^{19}F in FH, and even ^{23}Na in NaH and ^{7}Li in LiH are nearly superposable.

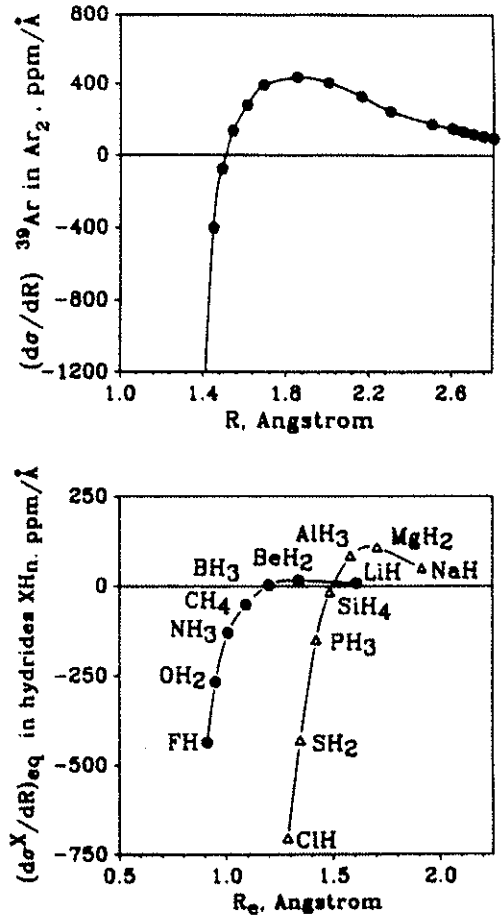

Fig. 13 Derivatives of the X nuclear shielding in XH_n vary with R_e in the same way as the shielding derivative function in Ar...Ar

Finally, we offer as evidence the variation of the sign of the derivative of the shielding at r_e, $(d\sigma/dR)_{eq}$ among the hydrides of the first two rows of the periodic table. The change in sign was first noted by Chesnut.[22] For both first- and second-row hydrides, the shielding derivative starts out to be positive and small at the alkali end of the periodic table. A slight increase in the shielding derivative is observed upon going to the hydrides of the alkaline earth metals. Then a decrease in the derivative is observed upon going to boron and aluminum hydrides. This drop in the shielding derivative continues on, such that at the halogen end of the Periodic Table, it is generally negative and large. Our explanation for these trends suggests itself when the equilibrium bond lengths in these hydrides are compared.[46] In Fig. 13 we plot the shielding derivatives $(d\sigma^X/dR)_{eq}$ vs. the equilibrium X-H bond length. The similarity between *inter*molecular and *intra*molecular shielding functions is clearly depicted by the similarity between the derivative function $d\sigma/dR$ vs. R for ^{39}Ar in Ar_2 and the $(d\sigma^X/dR)_{eq}$ vs. r_e for the XH_n hydrides. We propose that the shielding derivatives provide glimpses into the $\sigma(R)$ function at the specific values of R which are the equilibrium bond lengths, and these glimpses trace out the same shape as the one we have already found for the intermolecular $\sigma(R)$ and for ^{23}Na in NaH molecule.

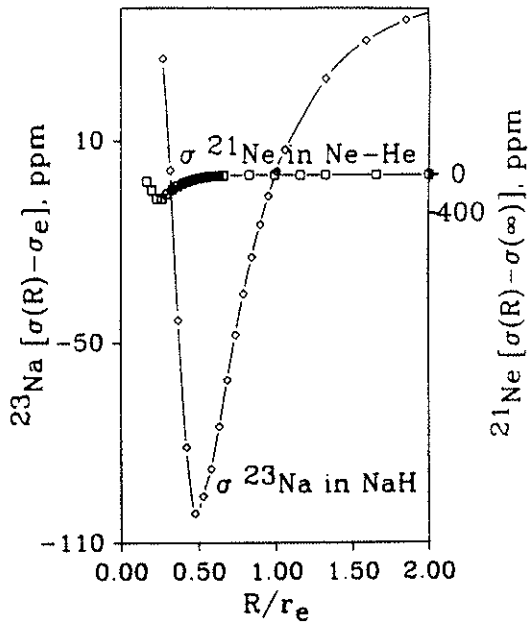

Fig. 14 Shielding surfaces in the isoelectronic systems NaH and Ne...He. The vertical scales are in the same ratio as $\langle a_0^3/r^3\rangle_{np}$ for ^{23}Na and ^{21}Ne atoms

In closing, we provide the proper perspective on the relative magnitudes of the changes in shielding with changes in interatomic distance in two-atom systems, the two can be compared if the $\langle a_0^3/r^3\rangle$ scaling of shielding sensitivity is taken into account. This is shown in Fig. 14 for the isoelectronic systems Ne...He and NaH. When ^{21}Ne is drawn on the ^{23}Na scale by using the respective $\langle a_0^3/r^3\rangle$ for the Ne and Na atoms for the vertical scales, we find that the intermolecular shielding changes are indeed much smaller than the intramolecular shielding changes.

ACKNOWLEDGMENT. The research described in this talk has been supported by the National Science Foundation (Grants CHE89-01426 and CHE92-10790). Professor

Thomas D. Bouman provided assistance in the SOLO calculations described here. His untimely death is a loss to all those interested in the elucidation of the nuclear magnetic shielding tensor.

References

1. Jameson, C. J., (1980) 'Effects of intermolecular interactions and intramolecular dynamics on nuclear resonance', Bull. Magn. Reson. 3, 3-28.
2. Jameson, C. J., Jameson, A. K., and Burrell, P. M. (1980) '^{19}F nuclear shielding scale from gas phase studies', J. Chem. Phys. 73, 6013-6020.
3. Hindermann, D. K. and Cornwell, C. D. (1968) 'Fluorine and proton NMR study of gaseous hydrogen fluoride', J. Chem. Phys. 48, 2017-2024.
4. Jameson, C. J., Jameson, A. K., Oppusunggu, D., Wille, S., Burrell, P. M., and Mason, J. (1981) '^{15}N nuclear magnetic shielding scale from gas phase studies', J. Chem. Phys. 74, 81-88.
5. Jameson, A. K., and Jameson, C. J. (1987) 'Gas phase ^{13}C chemical shifts in the zero-pressure limit: refinements to the absolute shielding scale for ^{13}C', Chem. Phys. Lett. 134, 461-466.
6. Wasylishen, R. E., Mooibroek, S., and Macdonald, J. B. (1984) 'A more reliable ^{17}O absolute chemical shielding scale', J. Chem. Phys. 81, 1057-1059.
7. Davies, P. B., Neumann, R. M., Wofsy, S. C., and Klemperer, W. (1971) 'Radiofrequency spectrum of phosphine (PH_3)', J. Chem. Phys. 55, 3564-3568.
8. Jameson, C. J., de Dios, A., and Jameson, A. K. (1990) 'Absolute shielding scale for ^{31}P from gas-phase nmr studies', Chem. Phys. Lett. 167, 575-582.
9. Wasylishen, R. E., Connor, C., and Friedrich, J. O. (1984) 'An approximate absolute ^{33}S nuclear magnetic shielding scale', Can. J. Chem. 62, 981-985.
10. Jameson, C. J. and Jameson, A. K. (1988), 'Absolute shielding scale for ^{29}Si', Chem. Phys. Lett. 149, 300-305.
11. Buckingham, A. D. and Pople, J. A. (1956) 'Electromagnetic properties of compressed gases', Faraday Soc. Discuss. 22, 17- 21.
12. Raynes, W. T., Buckingham, A. D., and Bernstein, H. J. (1962) 'Medium effects in proton magnetic resonance. I. Gases', J. Chem. Phys. 36, 3481-3488.
13. See for example, Jameson, C. J., Jameson, A. K., and Oppusunggu, D. (1986) 'Temperature dependence of ^{77}Se, ^{125}Te, and ^{19}F shielding and M-induced isotope shifts in MF_6 molecules', J. Chem. Phys. 85, 5480-5483.
14. Jameson, A. K., Jameson, C. J., and Gutowsky, H. S. (1970) 'Density dependence of ^{129}Xe chemical shifts in mixtures of xenon and other gases', J. Chem. Phys. 53, 2310-2321.
15. Jameson, C. J., Jameson, A. K., and Cohen, S. M. (1975) 'Temperature and density dependence of ^{129}Xe chemical shift in rare gas mixtures', J. Chem. Phys. 62, 4224-4226.
16. Jameson, C. J., Jameson, A. K., and Cohen, S. M. (1976) 'Second virial coefficient of ^{129}Xe chemical shielding in mixtures of Xe with spherical top molecules, CH_4, CF_4, and SiF_4', J. Chem. Phys. 65, 3401-3406.
17. Jameson, C. J. (1991) 'Rovibrational averaging of molecular electronic properties', in Z. B. Maksic (ed.), Theoretical Models of Chemical Bonding, Part 3. Molecular Spectroscopy, Electronic Structure, and Intramolecular Interactions, Springer-Verlag, Berlin, pp. 457-519.
18. Jameson, C. J. and Osten, H.-J. (1986) 'Theoretical aspects of the isotope effect on nuclear shielding', in G. A. Webb (ed.), Annual Reports on NMR Spectroscopy, Academic Press, London, Vol. 17, pp. 1-78.

19. Jameson, C. J., de Dios, A. C., and Jameson, A. K. (1991), 'Nuclear magnetic shielding of nitrogen in ammonia', J. Chem. Phys. 95, 1069-1079.
20. Riley, G., Raynes, W. T., and Fowler, P. W. (1979) 'The variation of molecular properties with vibration-rotation', Mol. Phys. 38, 877-892.
21. Fowler, P. W., Riley, G., and Raynes, W. T. (1981), 'Dipole moment, magnetizability, and nuclear shielding surfaces for the water molecule', Mol. Phys. 42, 1463-1481.
22. Chesnut, D. B. (1986) 'NMR chemical shift bond length derivatives of the first- and second-row hydrides', Chem. Phys. 110, 415-420.
23. Chesnut, D. B. and Wright, D. W. (1991) 'Chemical shift bond derivatives for molecules containing first-row atoms', J. Computational Chem. 12, 546-559.
24. Chestnut, D. B. and Foley, C. K. (1986) 'Chemical shifts and bond modification effects for some small first-row-atom molecules', J. Chem. Phys. 84, 852-861.
25. Ditchfield, R. (1981) 'Theoretical studies of the temperature dependence of magnetic shielding tensors: H_2, HF, and LiH', Chem. Phys. 63, 185-202.
26. Fleischer, U., Schindler, M., and Kutzelnigg (1987) 'Magnetic properties in terms of localized quantitities. VI. Small hydrides, fluorides, and homonuclear molecules of phosphorus and silicon', J. Chem. Phys. 86, 6337-6347.
27. Hegstrom, R. A. (1979) 'g factors and related magnetic properties of molecules. Formulation of theory and calculations for H_2^+, HD^+, and D_2^+', Phys. Rev. A 19, 17-30.
28. Lazzeretti, P., Zanasi R., Sadlej, A. J., and Raynes, W. T. (1987) 'Magnetizability and carbon-13 shielding surfaces for the methane molecule', Mol. Phys. 62, 605-616.
29. Raynes, W. T., Fowler, P. W., Lazzeretti, P., Zanasi, R., and Grayson, M. (1988) 'The effects of rotation and vibration on the carbon-13 shielding, magnetizabilities and geometrical parameters of some methane isotopomers', Mol. Phys. 64, 143-162.
30. Jameson, C. J., de Dios, A. C., and Jameson, A. K. (1991) 'The ^{31}P shielding in phosphine', J. Chem. Phys. 95, 9042-9053.
31. RPAC version 8.5, Thomas D. Bouman, Southern Illinois University at Edwardsville, and Aage E. Hansen, H. C. Oersted Institute, Copenhagen, Denmark.
32. Hansen, A. E. and Bouman, T. D. (1985) 'Localized orbital/local origin method for calculation and analysis of NMR shieldings. Applications to ^{13}C shielding tensors', J. Chem. Phys. 82, 5035-5047.
33. GAUSSIAN88, M. J. Frisch, M. Head-Gordon, H. B. Schlegel, K. Raghavachari, J. S. Binkley, C. Gonzalez, D. J. Fox, R. A. Whiteside, R. Seeger, C. F. Melius, J. Baker, R. Martin, L. R. Kahn, J. J. P. Stewart, E. M. Fluder, S. Topial, and J. A. Pople, Gaussian, Inc., Pittsburgh, PA. 1988.
34. Spirko, V., Stone, J. M. R., and Papousek, D. (1976) 'Vibration-inversion-rotation spectra of ammonia: centrifugal distortion, coriolis interactions, and force field in $^{14}NH_3$, $^{15}NH_3$, $^{14}ND_3$, and $^{14}NT_3$', J. Mol. Spectrosc. 60, 159-178.
35. Jameson, C. J. and Osten, H. J. (1985) 'Systematic trends in the variation of ^{19}F nuclear magnetic shielding with bond extension in halomethanes', Mol. Phys. 55, 383-395.
36. Stevens, R. M., Pitzer, R. M., and Lipscomb, W. N. (1963) 'Perturbed Hartree-Fock calculations I. Magnetic susceptibility and shielding in the LiH molecule', J. Chem. Phys. 38, 550-560.
37. Jameson, C. J. (1991) 'Gas phase NMR spectroscopy', Chem. Rev. 91, 1375-1395.
38. Rummens, F. H. A. (1975) 'Van der Waals forces and shielding effects', in P. Diehl, E. Fluck, and R. Kosfeld (eds.) NMR Basic Principles and Progress, Springer, Berlin, Vol. 10, pp. 1-118.